Cellulose
https://doi.org/10.1007/s10570-023-05585-y

ORIGINAL RESEARCH

Nanodiamond-treated flax: improving properties of natural fibers

Carsten Hinzmann · Drew F. Parsons · Johannes Fiedler · Justas Zalieckas · Bodil Holst

Received: 17 April 2023 / Accepted: 24 October 2023

Abstract Synthetic fibers are used extensively as reinforcement in composite materials, but many of them face environmental concerns such as high energy consumption during production and complicated decommissioning. Natural fibers have been considered as an attractive solution for making composites more sustainable. However, they are generally not as strong as synthetic fibers. It is therefore of interest to investigate ways to improve the properties of natural fibers without compromising environmental issues. Here, we present a study of the moisture absorption and mechanical properties of flax that has been exposed to hydrogenated nanodiamonds through an ultrasonic dispersion treatment. Nanodiamonds are known to be non-toxic, unlike many other carbon-based nanomaterials. We show that nanodiamond-treated flax fabric has a lower moisture content (~ −18%), lower moisture absorption rate and better abrasion resistance (~ +30%). Single yarns, extracted from the fabric, show higher tensile strength (~ +24%) compared to untreated flax. Furthermore, we present a theoretical model for the nanodiamond fiber interaction, based on the Derjgauin–Landau–Verwey–Overbeek (DLVO) theory of colloid interactions. The simulations indicate that the mechanical properties improve due to an enhancement of the electrolytic force, dispersion force and hydrogen bonding of nanodiamond-treated fibers, which strengthens the cohesion between the fibers. We also apply the model to nanodiamond-treated cotton. The lower zeta potential of cotton increases the electrolytic force. Comparing the results to experimental data of nanodiamond-treated flax and nanodiamond-treated cotton suggests that the fiber's zeta potential is critical for the improvements of their mechanical properties.

Graphical abstract

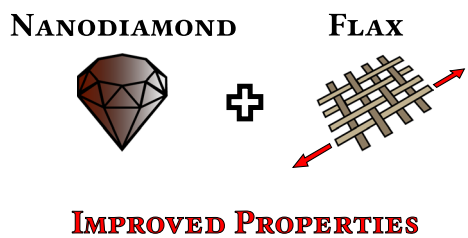

Keywords Flax · Nanodiamond · Tensile strength · Moisture content · Zeta potential · Dispersion force

Supplementary Information The online version contains supplementary material available at https://doi.org/10.1007/s10570-023-05585-y.

C. Hinzmann (✉) · J. Fiedler · J. Zalieckas · B. Holst
Department of Physics and Technology, University of Bergen, Bergen, Norway
e-mail: carsten.hinzmann@uib.no

D. F. Parsons
Department of Chemical and Geological Sciences, University of Cagliari, Cagliari, Italy

Published online: 01 December 2023

Introduction

Fiber reinforced polymer composites have a wide range of use because of their unique modularity. For example, boats and wind turbine blades have been made from glass fiber composites for decades. High-end applications that require maximum strength and minimal weight rely on carbon fibers for reinforcement. However, the production of synthetic fibers consumes a lot of energy (Huda et al. 2008; Peças et al. 2018; Wu et al. 2018). The demand for composite materials is increasing, and the amount of synthetic fiber waste is predicted to follow this trend (Khurshid et al. 2020; Naqvi et al. 2018). Natural fibers as reinforcement can be an environmental and sustainable alternative, which is superior to glass fibers regarding the specific strength, energy consumption and costs (Huda et al. 2008; Peças et al. 2018; Pil et al. 2016; Joshi et al. 2004).

However, natural fibers have drawbacks, such as non-uniformity, poor thermal stability, and limited mechanical strength. Another disadvantage for the application in composites is their relatively high moisture sorption and the resulting poor compatibility between the natural fibers (hydrophilic) and the matrix (hydrophobic). Therefore, different treatments for natural fibers were studied. Chemical treatments, like alkaline treatment, showed improved thermal stability, increasing tensile strength and better interfacial bonding in composites (Van de Weyenberg et al. 2006; Li et al. 2007; Nurazzi et al. 2021). Nanoparticles like carbon nano tube (CNT), graphene and nanodiamond were also used for treating natural fiber reinforcements. The treatment with CNTs showed improved mechanical and fracture properties of natural fiber composites (Kordkheili et al. 2013; Tzounis et al. 2014; Shen et al. 2014; Li et al. 2015). The application of CNT on single flax threads could increase the Young's modulus by 70% without improving the tensile strength compared to untreated flax (Li et al. 2015). Graphene-treated natural fibers showed improved thermal and mechanical properties, as well as better interfacial bonding in composites (da Luz et al. 2020; Sarker et al. 2018, 2019; Karim et al. 2021). Sarker et al. (2018) could improve the tensile strength on elementary jute fibers by 96% compared to untreated fibers with a hot water, alkali, and graphene oxide treatment. A follow-up investigation by Karim et al. (2021) performed the same treatment with reduced graphene oxide instead of graphene oxide and reached improvements of 176% in tensile strength compared to untreated fibers.

Nanodiamond has attracted considerable attention because of its excellent chemical and thermal stability, mechanical strength, and the ability of modulating its surface with functional groups (Schmidlin et al. 2012; Mochalin et al. 2012). Hydrogenated nanodiamonds have a positive zeta potential at neutral pH (Cicala et al. 2017; Arnault and Girard 2017), making it useful for seeding of negatively charged substrates for chemical vapor deposition (CVD) of diamond (Williams et al. 2010) and treatment of negatively charged surfaces in general.

Houshyar et al. (2019) treated plain cotton fabrics with nanodiamond, improving the thermal and mechanical properties for textile applications. A simple dip-coating procedure of the fabric in a water dispersion with a nanodiamond concentration of just 0.3% led to an increase in tensile strength by 40% and an increased abrasion resistance by 58% compared to untreated fabrics (Houshyar et al. 2019). This shows that only small amounts of nano-particles are needed for improving the fiber properties significantly. The non-toxicity is a major advantage of nanodiamond compared to other carbon-based nanomaterials (Mochalin et al. 2012).

Natural fibers vary naturally in length and are commonly spun to obtain continuous staple fiber yarns that can be processed to textiles and composite reinforcements. In the following the terms "yarn" and "thread" are used synonymously. Spinning introduces twist into the yarn which is the primary binding mechanism in conventional staple fiber yarns. The twist angle in the yarn can influence many yarn characteristics including yarn compaction, linear density and importantly, yarn strength (Shah et al. 2012). However, the optimal twist differs between textile and composite applications. For dry yarns, measurements show maximum strength at higher twist levels (Goutianos and Peijs 2003) and simulations confirm the critical importance of friction between the fibers for the yarn's strength (Van Langenhove 1997). In composites, low twist is preferable because of the better permeability of the yarns and less obliquity and misalignment of the fibers. This results in better mechanical properties and was shown in experiments (Goutianos and Peijs 2003; Baets et al. 2014) as well as models (Rao and Farris 2000; Shah et al. 2013).

Shah et al. (2012) demonstrated that a hydroxyethylcellulose surface treatment of natural fibers can be used to minimize the twist of yarns for composite applications. Their treatment of low twist flax yarns caused intra-yarn binding, which increased the friction between the fibers and strengthened the yarn by 230%.

Flax has been spun and woven to linen textiles for centuries (Hüster-Plogmann et al. 1997; Leuzinger and Rast-Eicher 2011) and is still popular for clothing because of its good breathing and moisture regulating properties. Therefore, the textile/clothing industry still has the highest demand for flax fibers (Baley et al. 2018). Abrasion is a main source for failure in textiles and has been improved with alkaline treatment, chemical crosslinking (Mccall et al. 2001) and silica treatment (Alongi and Malucelli 2013). Since the 1990s, flax is one the most used natural fibers for reinforcement in composites (Peças et al. 2018). Its main application is in the automotive sector, where non-load bearing parts are replaced to save weight and costs (Peças et al. 2018; Carus et al. 2015). Other possible applications for flax fiber-based composites are medical applications like implants (Kumar et al. 2020) and wound-dressing, supercapacitors, oil/water separation and building materials (Li et al. 2022).

In the research field of cellulose, hydrogen bonding is a common explanation for a large variety of phenomena and properties, such as mechanical strength of fibrils, fiber-fiber bonding or forming of paper. However, according to Wohlert et al. (2022) this explanation can be wrong (high axial modulus and strength of fibrils) or is often incomplete (fiber-fiber bonding, forming of paper), while in most cases the effect of moisture is neglected. Hydrogen bonds between nano-particles and natural fibers have also been proposed to explain the observed improvements in mechanical properties (Li et al. 2015; Houshyar et al. 2019; Hu et al. 2010). However, a theoretical study by Nishiyama (2018) suggested that it is the dispersion force (Scheel and Buhmann 2008) (induced dipole-induced dipole force) that is predominant (50–70%) in the cohesion of cellulose, which translates directly to plant-based natural fibers that mainly consist of cellulose. In addition, it has been proposed (Wohlert et al. 2022) that water/moisture plays an important role in fibril–fibril and fiber–fiber joints. Moisture sorption occurs primarily in the non-crystalline parts of the fiber, mainly hemicelluloses and lignins (Lu et al. 2022), that can be seen as a matrix for the unidirectionally oriented cellulose microfibrils (Müssig and Haag 2015). These non-cellulose materials are also mostly affected by swelling, which leads to a stronger expansion in transverse direction of the fiber and an increase in its diameter (Lu et al. 2022). In this process, water molecules fill voids in the three-dimensional shape of matrix/fibers and bridge hydroxyl groups of the fiber's components with hydrogen bonds (Wohlert et al. 2022). Therefore, the presence of water might contribute substantially to the fiber strength. Simulations by Zhang et al. (2021) on cellulose nanocrystals confirmed this hypothesis by showing that hydrogen bonds between the cellulose nanocrystals are 2.6 times stronger in wet conditions. Furthermore, experiments on flax showed that untreated flax has up to 23% higher tensile strength at a relative humidity of 66% compared to a relative humidity of 30% (Stamboulis et al. 2001).

The Derjgauin–Landau–Verwey–Overbeek (DLVO) theory of colloid interactions (Derjaguin and Landau 1941; Verwey and Overbeek 1948) has previously been applied to the interactions of cellulose (Fukuzumi et al. 2014) and nanodiamond (Sychev et al. 2017) materials in aqueous environments, for instance addressing cellulose interacting with quartz (Hartmann et al. 2018) and titania (Siffert and Metzger 1991) minerals. DLVO theory models the total interaction force as the sum of electrolytic force arising from electrolyte ions adsorbing to charged surfaces, together with macroscopic van der Waals (dispersion) force driven by the dielectric polarizability of particles and medium. This is discussed in detail by Fiedler et al. (2023). The interaction between nano-particles and cellulose could be dominated by electrolytic and dispersion force and water-induced hydrogen bonds via absorbed moisture. To the best of our knowledge this has not been studied so far.

In this study, we present an investigation of the moisture absorption and mechanical properties of flax fabric treated with hydrogen-terminated nanodiamonds. Moreover, we present a theoretical explanation of our results by comparing the magnitude of DLVO forces against the strength of hydrogen bonds.

Table 1 Properties of technical flax fabric used in this study

Area density:	150 g m^{-2}
Weave pattern:	2/2-twill
Warp weave density:	25.4 threads cm^{-1}
Weft weave density:	24 threads cm^{-1}
Thread number metric:	36 Nm
Thread twist level:	670 tpm

Table 2 Properties of hydrogen-terminated nanodiamond water dispersion used in this study

Nanodiamond content:	2.5% (Myllymäki 2014)
Nanodiamond crystal size:	4–6 nm (Myllymäki 2014)
Zeta potential at pH 7:	50 mV (Myllymäki 2021)

Experimental methods

Materials

The materials used are all commercially available. A chemically untreated, technical flax fabric for composite making was supplied by Libeco NV, Belgium. Its properties are listed in Table 1. Hydrogen-terminated nanodiamonds dispersed in water (uDiamond® Hydrogen D) were supplied by Carbodeon Ltd Oy, Finland. Its properties are listed in Table 2.

Nanodiamond treatment

Flax fabric was cut into samples of 80 mm × 80 mm size and mounted on a sample holder consisting of a base metal plate and a top metal frame, clamping the ends of the flax fabric, see Fig. S1 in the supporting information (SI). Before fixing the flax fabric with the frame, it was wetted with water. Surface impurities were removed from the samples by using ultrasonic agitation (180 W, 45 kHz), first for 3 min in isopropanol and then for 20 min in deionized water. The nanodiamond dispersion was diluted with deionized water from a nanodiamond content of 2.5 to 0.3%. The cleaned flax samples were dip-coated in the dispersion for 30 min using ultrasonic agitation (180 W, 45 kHz). After the treatment, the flax fabrics were rinsed with deionized water to remove nanodiamond agglomerates and residual impurities. Then, the samples were dried for at least 6 h on a hotplate at 60 °C to evaporate water without degrading the flax (Van de Velde and Baetens 2001). The reference samples were prepared the same way as the nanodiamond-treated samples, except for the nanodiamond treatment. In total, three nanodiamond-treated samples and three reference samples were made.

Characterization

Scanning electron microscopy (SEM)

Untreated and nanodiamond-treated flax were cut in each case into a circular piece of fabric with a diameter of 20 mm. Figure 1 shows the fixed samples that were imaged with a Zeiss Supra 55 VP SEM without any sample coating. An Everhart–Thornley (ET) detector was used at a bias of 200 V with an acceleration voltage of 2.5 kV to come close to the charge balance with the uncoated sample (Flatabø et al. 2017).

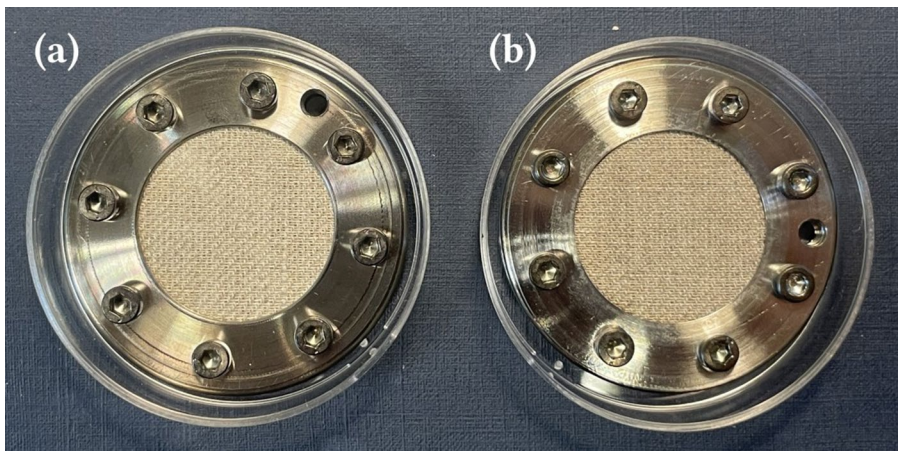

Fig. 1 Image of untreated flax (**a**) and nanodiamond treated flax (**b**) fixed for scanning electron microscopy (SEM) imaging; Nanodiamonds absorb visible light and cause the nanodiamond-treated flax fabric to appear darker in comparison to untreated flax

Quantitative assessment of the nanodiamond uptake

The nanodiamond uptake of the flax fabric after treatment was measured with an analytical balance (KERN & SOHN GmbH, ABT 220-4M). Flax fabric was cut into samples of 260 mm × 450 mm size and prepared as described in Sect. 2.2. After cleaning the samples, an additional drying step at 60 °C for at least 6 h was included. The dry flax was weighed before and after nanodiamond treatment. The standard mode of the balance was used. The weighing was performed immediately after the drying to minimize moisture uptake from the air. In total, three samples were made.

Moisture content and absorption rate

The moisture content and absorption rate of untreated and nanodiamond-treated flax were measured with an analytical balance (KERN & SOHN GmbH, ABT 220-4M). The nanodiamond treatment is described in Sect. 2.2. Untreated and nanodiamond-treated flax fabric of 260 mm × 450 mm size were dried on a hot plate at 60 °C for removing moisture only (Van de Velde and Baetens 2001). The drying time was around 1 h to reach a lower water equilibrium than at room temperature. The average temperature in the laboratory was (22 ± 1)°C and the average relative humidity was (24.4 ± 0.4)%. The mass of the flax was measured before the drying and monitored after the drying to measure the moisture content and the relative water absorption rate from the surrounding air. The measurement was performed two times for each fabric.

Mechanical tests

Martindale abrasion resistance tests were performed based on BS EN ISO12947-2:2016 by Shirley Technologies Limited, United Kingdom. The tests were conducted using a Martindale abrasion machine with a head loading of (12.0 ± 0.3) kPa and the standard wool worsted crossbred reference abradant fabric. The number of abrasion cycles was counted until the observation of the complete breakage of at least two separate threads in the weave construction.

Tensile strength tests were performed based on BS EN ISO13934-1:2013 by Shirley Technologies Limited, United Kingdom. A constant rate of extension (CRE) tensile testing machine was used for this purpose. A length of thread extracted from the fabric is gripped perpendicularly in the clamps of the machine. Tensile force is applied in the direction of the length of the thread at a jaw speed of 100 mm min^{-1}. The initial clamping length was 20 mm. Tests were carried out on ten separate pieces of thread extracted from the fabric warp and weft directions. The maximum breaking force and the elongation at maximum force were measured. The BS EN ISO139 standard conditions for temperature and relative humidity were met with (19.3 ± 0.3)°C and (66 ± 2)%, respectively.

All equipment used during the tests is calibrated externally in accordance with the ISO 17025 quality management system that is accredited to Shirley Technologies Limited, United Kingdom.

Results and discussion

Surface properties of flax fibers

Figure 2 shows SEM images of the flax fabric (a), a single thread (b), the surface of an untreated elementary fiber (c) and the surface of a nanodiamond-treated elementary fiber (d). The difference in diameters of warp (thin, vertical) and weft (thick, horizontal) threads of the twill fabric is visible in Fig. 2a. This difference is due to the weaving process, which yields higher loads on warp threads (Barella 1950; Rukuiziene and Kumpikaite 2013) and can be seen in the higher warp weave density, too, having more warp threads within a centimeter than weft threads.

The surface of nanodiamond-treated flax (Fig. 2d) appears rougher than the untreated flax surface (Fig. 2c). We attribute the increased roughness seen in Fig. 2d to the nanodiamond treatment. However, the SEM resolution is not high enough to identify with certainty nanodiamonds of a few nano-meter size. Nanodiamonds tend to aggregate (Krüger et al. 2005; Yoshikawa et al. 2015) and the structure seen may be the aggregation of nanodiamonds. Alternatively, the rougher surface could be the result of abrasion with the nanodiamonds during ultrasonic agitation.

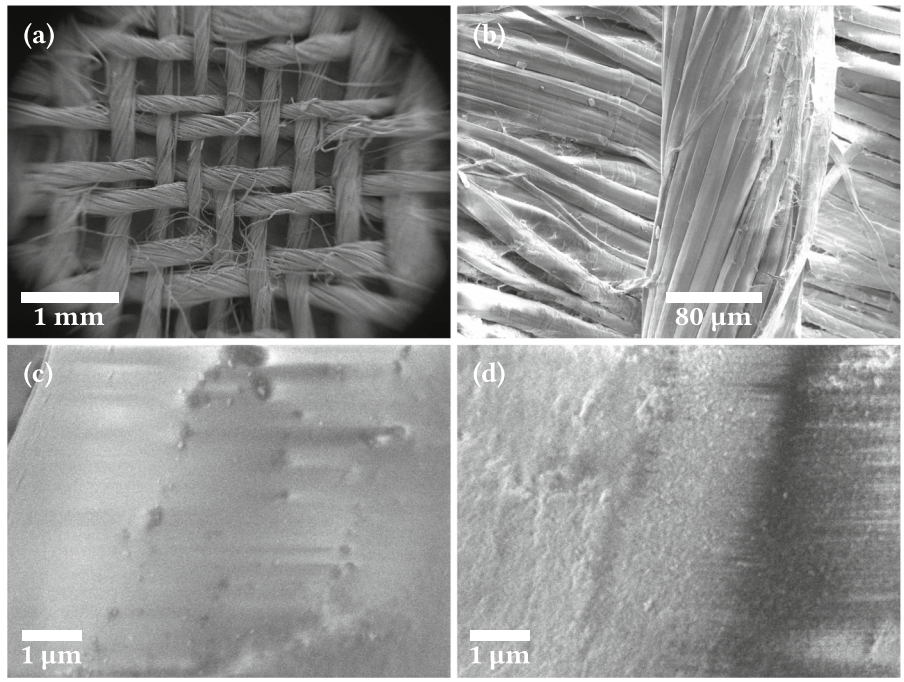

Fig. 2 SEM pictures of flax; Flax fabric (**a**), single thread (**b**), the surface of an untreated elementary fiber (**c**) and the surface of a nanodiamond-treated elementary fiber (**d**); See Sect. 2.3.1 for instrument settings and sample preparation

In Fig. 1, a difference in color between untreated flax, Fig. 1a, and nanodiamond treated flax, Fig. 1b, is visible. Nanodiamonds have a strong optical absorption in the visible part of the spectrum, due to the graphitization of the nanodiamond surface during its formation. This gives nanodiamonds and its dispersions a dark-brown color (Vul et al. 2014). The darker, slightly browner color of the nanodiamond treated fabric, Fig. 1b, is therefore a strong indication that the nanodiamonds are bonded to the flax fibers through the treatment. Even rinsing the nanodiamond-treated fabric after the treatment did not change its darker appearance.

Nanodiamond density

Knowing the nanodiamond density can be helpful to evaluate the nanodiamond treatment of a material. A quantification of the nanodiamond density through the difference in color between the untreated and nanodiamond treated flax, Fig. 1, is not feasible. Moreover, single nanodiamonds could not be resolved by SEM, Fig. 2, which prevents an accurate quantification of their area density. However, the nanodiamond uptake could be determined by measuring the weight of a large piece of flax fabric before and after the nanodiamond treatment. This information was used for approximating the area density of nanodiamonds on the fibers, ρ_{ND}. A simple model for the number of nanodiamonds bonded to the flax fabric and the sample surface area was developed. Here, nanodiamonds, which are cuboctahedron in shape (Vul et al. 2014) are approximated as spheres and elementary flax fibers, which generally have a polygonal cross section (Lukesova and Holst 2021) are approximated as cylinders for simplification. Further details on the model are described in the SI, Section S3.

The results of the nanodiamond mass measurements and the estimates of the nanodiamond density are summarized in Table 3. The high mass of nanodiamonds suggests that not only the surface of the fabric is fully covered by nanodiamonds, but also the elementary fibers within the yarns of the fabric. The maximal possible area density can be estimated as a function of the nanodiamond radius r_{ND} and is given by $\left(\sqrt{3}r_{ND}\right)^{-1}$ (Mandal 2021). For $r_{ND} = (2.5 \pm 0.5)\,\text{nm}$ the density is $(4.6 \pm 2.8) \cdot 10^{12}\,\text{cm}^{-2}$, which is in good agreement with the results of the model presented in this work. Assuming the aggregation of nanodiamonds, which is a well-known effect (Krüger et al. 2005; Yoshikawa et al. 2015), the size of the bonded

Table 3 Nanodiamond uptake measurement and area density calculation results

#	1	2	3
Fabric mass before (g)	14.2178	14.4663	14.2680
Fabric mass after (g)	14.2182	14.4976	14.3073
Nanodiamond mass (mg)	(0.4 ± 0.2)	(31.3 ± 0.2)	(39.3 ± 0.2)
N_{ND}	$(1.8 \pm 1.4) \cdot 10^{15}$	$(1.4 \pm 0.9) \cdot 10^{17}$	$(1.7 \pm 1.0) \cdot 10^{17}$
A_f (m^2)	(0.104 ± 0.001)	(0.105 ± 0.001)	(0.104 ± 0.001)
A_s (m^2)	(2.1 ± 0.6)	(2.2 ± 0.6)	(2.1 ± 0.6)
ρ_{ND} (cm^{-2})	$(8 \pm 7) \cdot 10^{10}$	$(6 \pm 4) \cdot 10^{12}$	$(8 \pm 5) \cdot 10^{12}$

The precision of the balance is ±0.1 mg; Area density of nanodiamonds $\rho_{ND} = N_{ND} A_s^{-1}$, with N_{ND} being the number of bonded nanodiamonds and A_s describing the surface area of all elementary fibers in the thread, which is a multiple of the area of the flax fabric A_f

Table 4 Moisture content of untreated and nanodiamond(ND)-treated flax after drying at 60 °C for around 1 h

	Untreated	ND-treated
Mass before drying (g)	(15.709 ± 0.009)	(14.991 ± 0.005)
Mass after drying (g)	(15.275 ± 0.006)	(14.646 ± 0.003)
Water mass (mg)	(434 ± 11)	(345 ± 6)
Moisture content	2.8%	2.3%

The moisture content of nanodiamond-treated flax is about 18% less than of untreated flax. The precision of the balance is ±0.1 mg

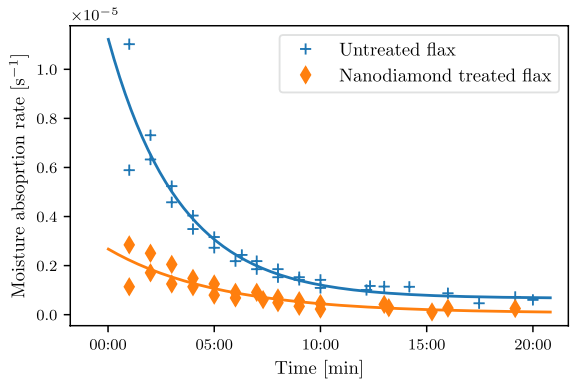

Fig. 3 Moisture absorption rate of untreated and nanodiamond-treated flax as a function of time after the drying on a hot plate at 60 °C; The data was fitted with an exponential function $f(t) = a \cdot e^{-bt} + c$, the fitting parameters are listed in Table S1; The moisture absorption rate of nanodiamond-treated flax is lower than of untreated flax at all times, leading to lower moisture content; Error bars are too small to be shown in the diagram

nanodiamonds can be a multiple of the size of a single nanodiamond. This means that the nanodiamond density is likely to be lower than the calculated ρ_{ND}. Therefore, ρ_{ND} can be interpreted as a maximal density.

The nanodiamond densities for sample 2 and 3 agree within one standard deviation. However, sample 1 deviates from the others by roughly two orders of magnitude. We assume that the reference sample contained more water than the nanodiamond-treated sample, yielding a too low nanodiamond mass. An unequal drying time before and after the nanodiamond treatment might have led to this inconsistency.

Even though a comparison between different materials is difficult, the estimated densities are consistent with reported densities of $\sim 10^{11}$ cm^{-2}, demonstrated with ultrasonic seeding techniques on silicon wafers (Mandal 2021; Williams et al. 2007).

Moisture content and absorption rate

Since high moisture sorption of natural fibers is one of their biggest drawbacks, it was tested if the nanodiamond treatment has an effect on the moisture content and absorption rate of flax. The results of the moisture content measurements of untreated and nanodiamond-treated flax are listed in Table 4. The nanodiamond treatment of flax reduces the moisture content of flax by about 18% compared to untreated flax. Calculation details can be found in the SI, Section S4. In a previous study the moisture content of untreated flax was measured to (10 ± 1)%, following the ASTM

D 2654-89 a:1998 standard (Surina and Andrassy 2013). These higher values can be explained by the higher relative humidity of about 65% in the standardized test.

In Fig. 3 the moisture absorption rate of untreated and nanodiamond-treated flax is shown as a function of time after the drying. The moisture absorption rate of nanodiamond-treated flax is lower than that of untreated flax at all times. Thus, the nanodiamond treatment not only reduces the moisture content of flax, but also delays the absorption of moisture after being dried. This might be explained by the hydrophobic nature of hydrogenated nanodiamonds that was shown experimentally (Stehlik et al. 2016; Vervald et al. 2019). The nanodiamond density estimates from Sect. 3.2 suggest a fully covered flax fiber surface. Similar to rain wear impregnation, the hydrophobic nanodiamonds could make the fiber absorb less moisture.

Mechanical properties

Abrasion resistance tests were performed on two samples of untreated and nanodiamond-treated flax fabric. It was found that the untreated flax samples could withstand more than 3000 and 4000 cycles, respectively, whereas both of the nanodiamond-treated flax samples withstand more than 5000 cycles. Thus, the nanodiamond treatment increased the abrasion resistance of flax by about 1500 cycles on average, corresponding to an improvement of about 30%. The results show that the treatment with nanodiamonds makes flax more resistant to mechanical wear. This is consistent with the work of Houshyar et al. (2019) on nanodiamond-treated cotton, which reports an increase in abrasion resistance by 58%. However, Houshyar et al. (2019) did not define a clear counting endpoint and based the abrasion cycle number on a subjective, visual judgment of the fabric, which is difficult to reproduce. Even though the dispersion concentration of 0.3% was the same during the nanodiamond treatment (Houshyar et al. 2019), cotton might see a stronger effect because of the different chemical composition compared to flax. This might influence the amount and density of nanodiamonds being bonded to the fiber and affect the abrasion resistance. However, in comparison to previously reported treatments for increasing the abrasion resistance, the nanodiamond treatment of flax shows a lower improvement. Mccall et al. (2001) could increase the abrasion resistance of flax fabric by a factor of three with a combination of an alkaline and crosslinking treatment.

Table 5 Mechanical properties of untreated (F) and nanodiamond-treated flax (F_{ND}); Mean values and standard deviation are presented for warp and weft threads

	Fabric	Breaking force (N)	Elongation at break (%)
Warp	F	(10 ± 2)	(8 ± 2)
	F_{ND}	(12 ± 4)	(7 ± 2)
Weft	F	(11 ± 3)	(7 ± 1)
	F_{ND}	(11 ± 4)	(6 ± 2)
Total	F	(10 ± 3)	(7 ± 2)
	F_{ND}	(12 ± 4)	(7 ± 2)

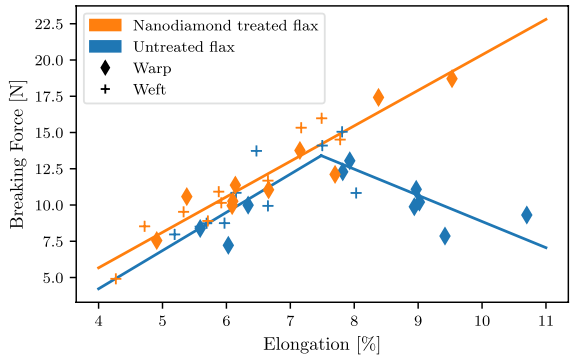

Fig. 4 Tensile strength as a function of elongation at break; The data was fitted with linear functions to visualize the general findings; Almost all tested nanodiamond-treated flax fibers are stronger than untreated flax fibers with the same elongation at break; Relative error in force is about 0.6%; Error bars are too small to be shown in the diagram

Tensile strength tests were performed on single threads that were extracted from the fabrics of untreated and nanodiamond treated flax. In this way fabric effects like interactions between threads in the fabric could be excluded, which simplifies the study of the nanodiamond treatment. The force-strain measurement raw data of untreated and nanodiamond-treated flax threads is shown in Fig. S2 in the SI. All tested threads show the typical force-strain curve of a brittle break during the elastic deformation that was reported previously for flax fibers (Bos et al. 2002; Charlet et al. 2009). The breaking force and elongation at break are summarized in Table 5, showing

the results for untreated and nanodiamond-treated flax threads in warp and weft directions. According to Shirley Technologies, who performed the tests, the relative error in force is about 0.6%.

Plotting the breaking force at the elongation at break of each tested single flax thread as shown in Fig. 4, reveals two interesting results. Firstly, only the data of untreated flax is split into two regimes, separated by the breaking force maximum between 7 and 8% elongation. It is striking that regime 2 (above 7–8%) consists almost exclusively of warp yarns. Secondly, a clear effect of the nanodiamond treatment is visible with a positive offset of breaking force values, showing that the treatment strengthens the flax.

On the first point. In regime 1 (below 7–8%) the breaking force increases with elongation and in regime 2 it decreases. This indicates that there are two failure mechanisms for untreated flax, which likely is related to the twist in the yarn and the clamping conditions during the tensile test. When the clamping length in tensile tests exceeds the elementary fiber length, not all elementary fibers in the yarn can be clamped at both ends. Thus, the yarn strength is more dependent on the cohesion between the elementary fibers, which results in less strength and higher elongations compared to tensile tests on single elementary fibers. This is also known as bundle effect (Bos et al. 2002; Sarker et al. 2018). Elementary flax fibers have a natural variation in length from 4 mm to 140 mm (Müssig and Haag 2015) with a mean value around 30 mm (Bos et al. 2002). Twist is the primary binding mechanism in staple fiber yarns and introduces friction between the fibers. The resulting inter-fiber cohesion prevents the fibers from slippage under tensile load. With increasing twist however, the probability of fiber breakage raises because of fiber obliquity, leading to a reduced yarn strength in tensile direction. Shah et al. (2013) showed that the surface twist angle of yarns is the important parameter to define twist and that maximum strength is reached at the twist angle at which both failure mechanisms, fiber slippage and fiber rupture, balance. We conclude, that the failure mechanism in regime 1 is dominated by fiber rupture, a simultaneous break of the elementary fibers, causing lower elongation at break. In regime 2, the failure mechanism is more dominated by slippage of elementary fibers, which can explain the higher elongation at break and the decreasing strength with elongation. The variability in measured strength at a certain elongation however, is likely due to the elementary flax fibers that have a coefficient of variation in the range from 20 to 60% (Aslan et al. 2011).

The fact that regime 2 almost exclusively consists of warp yarns is also related to twist and can be shown by modeling the structure of twisted fiber yarns (Rao and Farris 2000). Approximating the yarn as a cylinder, the twist surface angle, α, is depended on the yarn diameter, d, and is given by $\tan\alpha = \pi d T$. T is the twist level and defines the number of twist per meter. The lower diameter of warp yarns (see Sect. 3.1) results in a lower twist angle. This decreases the inter-fiber friction and leads to more fiber slippage, less strength and higher elongations in the tensile test.

On the second point. The breaking force of nanodiamond treated flax increases steadily with elongation and is higher than of untreated flax for almost all elongation values. The data (Fig. 4) was fitted with linear functions, interpolating the data points. This allows a quantified comparison between the breaking force of nanodiamond-treated flax and untreated flax at the same elongation, reflecting the precision of the measurements. It shows that in regime 1, the breaking force increased by (1 ± 1)N on average for nanodiamond-treated flax compared to untreated flax, while in regime 2, it increased by (5 ± 4)N, reflecting the strong effect of the nanodiamond treatment at high elongations. This is a significant enhancement of the tensile strength, yielding a maximum increase of about 47% in regime 1 and about 141% in regime 2. On average, the nanodiamond treatment increased the breaking force by more than 24% and decreased the elongation by about 11%.

We propose that the significant improvement in the flax's mechanical properties is a result of the nanodiamonds bonding to the flax fibers (see Sect. 3.1) and increasing the cohesion between the elementary fibers. The added friction and resistance to fiber slippage increases the tensile strength of nanodiamond treated flax and explains the absence of regime 2 in the breakage of nanodiamond treated flax (see Fig. 4). Fig. 5 shows a schematic of possible interactions between nanodiamonds, water and the elementary fibers of a flax thread. We suggest that the increased cohesion originates from an interplay between electrolytic forces, dispersion forces, direct hydrogen bonds, and indirect, water-induced hydrogen bonds.

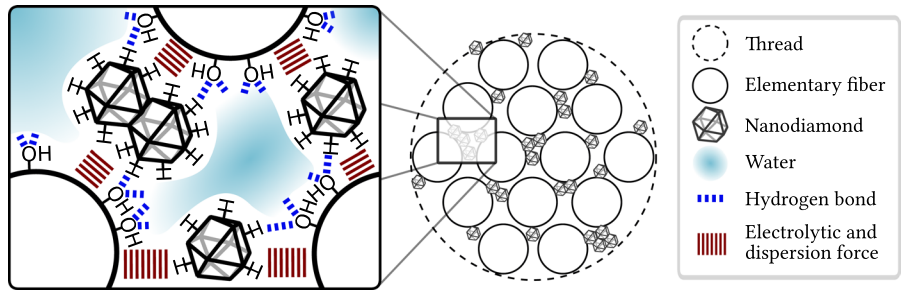

Fig. 5 Schematic (not to scale) of a thread's cross-section; Nanodiamonds bond between elementary fibers, increasing the cohesion between the elementary fibers and strengthening the thread; Additional water is confined by the hydrophobic nanodiamonds to further increase the cohesion between the elementary fibers

To explain our observations, we developed a model on the interaction of nanodiamonds and natural fibers/cellulosic materials. We applied the model to flax and cotton and compared the results to our experimental data on flax and previously published data on cotton (Houshyar et al. 2019).

Briefly, a DLVO model (Derjaguin and Landau 1941; Verwey and Overbeek 1948; Liang et al. 2007) of particle interactions is employed, calculating electrolytic forces and dispersion forces. The electrolytic interaction originates from opposite polarities and accounts for the formation of an ion adsorption layer at nanodiamond and natural fiber surfaces, i.e. physisorption of ions from the aqueous medium. The nanodiamond and flax/cotton surfaces with a constant surface charge density are calibrated against zeta potential measurements, resulting in their respective surface charges. More details on the electrolytic interaction model can be found in the SI in Section S6. Untreated, raw flax fibers with zeta potential −5mV in 1mM KCl (pH 7) (Bismarck et al. 2002) were modeled as flat surfaces with a constant surface charge of $-4.3 \cdot 10^{-4}\,\mathrm{cm}^{-2}$. Untreated, raw cotton fibers with zeta potential −15 mV in 1mM KCl (pH 7) (Pusić et al. 1999) were modeled as flat surfaces with a constant surface charge of $-13.1 \cdot 10^{-4}\,\mathrm{cm}^{-2}$. Nanodiamonds were modeled with constant surface charge generating a zeta potential of 40 mV in pure water (pH 7) (Williams et al. 2010). We tested two nanodiamond models: as a flat surface with charge $-3.6 \cdot 10^{-5}\,\mathrm{cm}^{-2}$ (referred to as *low* charge), and as a 4 nm diameter sphere with charge $0.02\,\mathrm{cm}^{-2}$ (referred to as *high* charge) (both generate 40 mV zeta potentials within their respective geometries). The dispersion force is calculated as the superposition of the Casimir force (Burger et al. 2020; Fiedler et al. 2020a) between the fibers and the medium-assisted Casimir–Polder force (Fiedler et al. 2017, 2019) between the fibers and nanodiamonds of 4 nm diameter. Here, we use the dielectric function for carbon from Bergström (1997), for water from Fiedler et al. (2020b) and for cellulose from Thiyam et al. (2015). More details on the dispersion interaction model can be found in the SI in Section S7.

The results of the simulation are shown in Fig. 6. The electrolytic force and dispersion force between nanodiamonds and flax fibers are shown in Fig. 6a, the electrolytic force and dispersion force between nanodiamond and cotton fibers are shown in Fig. 6b, both as a function of the fiber-nanodiamond-distance. Figure 6c compares flax to cotton in terms of the total force, the superposition of the electrolytic force and the dispersion force, as a function of the fiber-nanodiamond-distance.

The electrolytic force is long-ranged (100s of nm) and causes attraction between the nanodiamonds and the fiber (negative force), as well as repulsion (positive force) at short distances. For flax, the equilibrium point of zero force is at about 10 nm for the *high* charge and at about 300 nm for the *low* charge estimate. The *high* charge estimate has a stronger attraction and a stronger repulsion than the *low* charge estimate. The dispersion force is short-ranged (nm) and shows strong attraction at distances of less than 10 nm.

The total force, Fig. 6c, yields attraction between nanodiamonds and flax fibers at distances below 1 and 4.5 nm for the *high* and *low* charge estimates, respectively. The repulsion barrier with its maximum at about 2.5 nm might be overcome by the

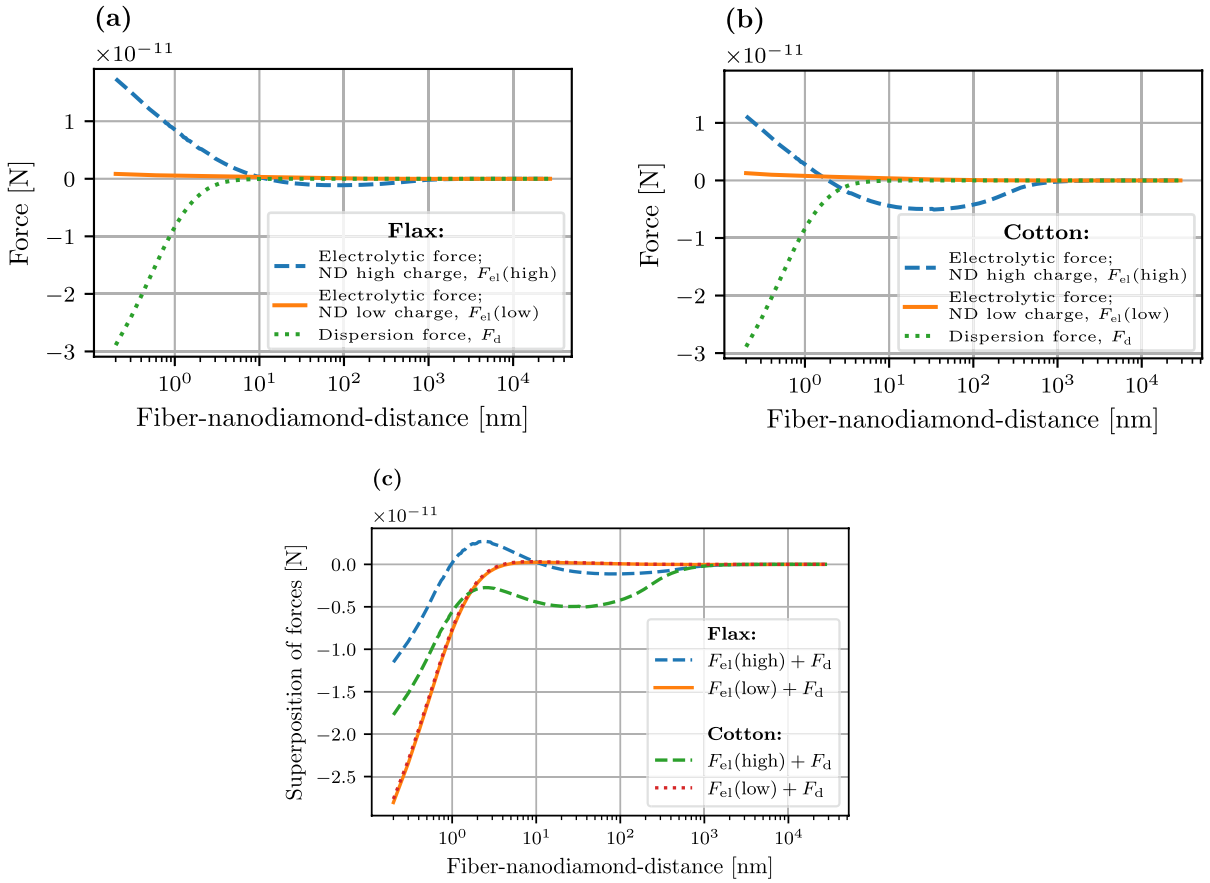

Fig. 6 Simulations of the electrolytic force (F_{el}) and dispersion force (F_d) between nanodiamonds (ND) and natural fibers as a function of fiber-nanodiamond-distance; (a) Nanodiamond-treated flax and (b) Nanodiamond-treated cotton; NDs are modeled as sphere with charge 0.02 cm^{-2} (*high*) and as a flat surface with charge $3.6 \cdot 10^{-5}$ cm^{-2} (*low*); (c) Superposition of electrolytic force and dispersion force as a function of fiber-nanodiamond-distance; The attraction at low distances might be a reason for the improved mechanical properties of nanodiamond-treated natural fibers; The total interaction between nanodiamond and cotton is stronger than between nanodiamond and flax, due to the lower zeta potential of cotton; For a more detailed explanation, see the main text and the calculations in the SI

ultra sonic agitation during the nanodiamond treatment, bringing the nanodiamonds close enough for bonding to the flax. This shows that nanodiamond induced electrolytic and dispersion forces contribute to increased cohesion between the flax fibers in nanodiamond treated yarns, which leads to the increase in tensile strength shown in Fig. 4.

Houshyar et al. (2019) reported an increase of 40% in tensile strength for nanodiamond-treated cotton fabric. This is a 67% greater improvement than the here reported 24% increase in tensile strength for nanodiamond-treated flax.

Our simulations, Fig. 6, show that the lower zeta potential of cotton leads to a stronger attractive electrolytic force for the *high* charge estimate, such that the repulsion is lower than for flax, the minimum of the attractive force well is deeper and the equilibrium point of zero force is at a lower distance, at about 2 nm. For the *low* charge estimate the repulsion of cotton is higher than for flax and the equilibrium point of zero force is at a longer distance. A direct comparison can be found in the SI, Fig. S3. Comparing the total force, the *low* charge estimate hardly shows any difference between cotton and flax. In the *high* charge estimate however, the total force of cotton is about − 0.5e−11 N shifted compared to flax, showing no repulsion barrier for cotton and just attractive interaction with the nanodiamonds. This results in a

54% greater attraction between cotton fibers and nanodiamonds compared to flax fibers and nanodiamonds at the minimum distance calculated of 0.2 nm.

These results suggest that the difference in zeta potential causes the different tensile strength improvements of nanodiamond treated cotton and flax . Even though it is in general not given that effects on a nano-scale, like the nanodiamond-fiber interaction, translate one to one to a macroscopic measure like the tensile strength, it is interesting to see that the relative difference in the simulated interaction of cotton and flax (54%) is in the same order of magnitude as the relative difference in measured tensile strength improvement (67%).

Furthermore, this relation draws two interesting implications, on the model itself and on the objective for improving the performance of natural fibers. On the one hand, it shows that the *high* charge estimate is the more relevant estimate for our model, since it reflects the difference between cotton and flax. On the other hand, the relation implies, that tuning the zeta potential of natural fibers might lead to huge improvements on the effect of nanodiamond treatments and further improve the fibers' mechanical properties.

Nevertheless, there are other possible contributions to the increase in tensile strength and the differences between flax and cotton, as well as limitations to our model. Starting with the experimental set-up, Houshyar et al. (2019) performed tensile tests according to the Australian Standard AS 2001.2.3.1-2001 on textile fabrics using the strip method. Due to the mechanical differences between fabric strips and fiber threads, these results are difficult to compare to the single thread tests presented in this work. For instance, the reported elongation at break of cotton strips (Houshyar et al. 2019) is more than three times higher than the elongation at break of single flax threads (see Table 5). This is likely originating from yarn interaction in the fabric strips.

Flax and cotton fibers are very different in many ways. Flax fibers, derived from the plant's stem, are round and straight, while cotton fibers are seed fibers that are flat, kinked and twisted (Ansell and Mwaikambo 2009). This different morphology could affect the nanodiamond interaction. Furthermore, the different chemical composition of flax and cotton can also have an influence on the nanodiamond treatment and the results. For instance the amount of cellulose in cotton is about 20% higher than in flax (Ansell and Mwaikambo 2009). This difference affects the moisture sorption and swelling of fibers and their zeta potentials (Bismarck et al. 2002). Even though this is considered in the electrolytic force model with the zeta potential dependency, the chemical composition is not implemented in the dispersion force model. Adding this information could further refine the results.

As indicated in Fig. 5, water is likely contributing to the increase in tensile strength of nanodiamond-treated fibers. Hydrogen-terminated nanodiamonds confine water (4.4% of the nanodiamond mass) (Stehlik et al. 2016), which can bridge small voids via hydrogen bonds between adjacent elementary fibers, strengthening the yarn. The importance of water as a mediator for bonds in cellulose and cellulose-based materials is discussed by Wohlert et al. (2022). For comparison, the strength of hydrogen bonds between cellulose crystals is reported to be $-1.3 \cdot 10^{-10}$ N in dry conditions $-4.7 \cdot 10^{-10}$ N in wet conditions with cellulose–water–cellulose hydrogen bonds (Zhang et al. 2021). It might be the dispersion forces that bring the nanodiamonds/fibers close enough for hydrogen bonding, which is reported to occur at distances of less than 0.35 nm (Cintrón et al. 2017). Since the direct and indirect hydrogen bonds are one order of magnitude stronger than the dispersion forces, it might be a combination of both of them that compensate for the electrolytic repulsion and improve the cohesion between the elementary fibers.

There is a strong analogy between the structure of twisted fibers in yarns and cellulose microfibrils in the secondary layer of elementary flax fibers. Both define the strength of the structure and the angle of their orientation with respect to the main yarn/fiber axis is very important (Müssig and Haag 2015). Because of their small size of a just few nanometers, it is conceivable that nanodiamonds could be transported into the elementary fibers by water sorption and swelling of the flax fibers during treatment. Flax fibers have a hierarchical structure, where cellulose microfibrils form macrofibrils and macrofibrils form layers around the lumen. On each level, the fibrils are embedded in a matrix of hemicellulose and lignin, which are prone to water sorption and swelling (Lu et al. 2022). On each of these levels, the interaction of nanodiamonds with fibrils could be similar to the depicted interaction with fibers in Fig. 5 and increase the fiber strength. Considering the similar scale of

nanodiamonds and fibrils, it is likely that interaction happens at the fibril level. The central issue is how permeable the flax fibers and their layers are for nanodiamonds. Tensile tests on single elementary fibers could provide new insides.

Comparing the nanodiamond treatment of flax presented in this work with a previously reported nano-particle treatment shows different improvements in the mechanical properties. Karim et al. (2021) reported that the treatment of elementary jute fibers with reduced graphene oxide can improve the tensile strength by about 176% compared to the untreated fibers. Jute fibers are naturally weaker than flax fibers due to a higher presence of noncellulosic materials such as hemicellulose, pectin, and lignin (Sarker et al. 2018). A hot water and alkali treatment removed these noncellulosic materials and decreased, together with the reduced graphene oxide treatment, the fiber diameter by about 34.5% (Karim et al. 2021). When expressed as force per cross-section area, this decrease in diameter alone leads to an increase in tensile strength in the order of the overall improvement, due to the quadratic dependency of the cross-section area on the diameter. Moreover, Karim et al. (2021) tested elementary fibers individually, in contrast to the here presented test of a flax thread/fiber-bundle. Elementary fibers alone are up to 50% stronger than in a bundle due to the bundle effect (Bos et al. 2002; Sarker et al. 2018), which might explain the lower increase in tensile strength for nanodiamond-treated flax presented in this work. However, just the fact that different plant fibers were tested can make a huge difference as discussed in the case of cotton and flax. A direct comparison of the same plant fiber with different treatments or the same treatment on different plant fibers is highly desirable and as important as equal testing conditions to draw final conclusions.

Nanodiamond treated flax shows potential for a series of applications. The increased abrasion resistance of flax fabric and increased tensile strength of flax yarn, can be directly applied to improve the durability of textiles, especially, since nanodiamonds are non-toxic. Furthermore, the presented nanodiamond treatment might help to close the performance gap between flax and glass fiber reinforced composites, which would open up new opportunities for lighter and stronger sustainable composites. Similar to the hydroxyethylcellulose treatment presented by Shah et al. (2012), the increased cohesion between fibers through the nanodiamond treatment can reduce the twist angle of flax yarn used in composite applications. As shown by Goutianos and Peijs (2003), minimal twist in flax fiber yarns results in the strongest composites. In addition, the presented positive effect on the moisture content suggests improvements in interfacial adhesion between nanodiamond treated flax and matrix materials, similar to natural fibers treated with graphene (da Luz et al. 2020; Sarker et al. 2018, 2019; Karim et al. 2021). This could be tested by single fiber fragmentation tests and single fiber pullout test (Brodowsky and Hennig 2021). Impregnating fiber bundles and performing standard tests (e.g. ASTM D3039 for tensile properties) is further needed to evaluate the performance of the nanodiamond treatment in the composite application.

Conclusions

In this work, we show that the treatment of flax fabric with nanodiamonds improves the abrasion resistance (~ +30%) and lowers the moisture content (~ −18%) and moisture absorption rate. Tensile tests on single yarns, extracted from nanodiamond treated fabric, show improved ultimate strength (~ +24%) compared to untreated flax. Furthermore, we present simulations indicating that the nanodiamonds enhance the cohesion between the elementary fibers of the flax threads, which improves the mechanical properties of flax. Our simulations suggest that the adhesion between the nanodiamonds and flax is a combination of electrolytic forces, dispersion forces, direct hydrogen bonds, and indirect, water-induced hydrogen bonds. Moreover, applying our model to nanodiamond-treated cotton and comparing the results to experimental data suggests that the fiber's zeta potential is critical for improvements of their mechanical properties. However, further experiments on natural fibers or other cellulosic materials with tuned zeta potentials are needed to test this hypothesis. In addition, further modeling is preferable to quantify all contributions to the adhesion between nanodiamonds and natural fibers. For instance, atomistic simulations of the friction force between nanodiamonds and cellulose based on the work of Zhang et al. (2021) could provide new insights on hydrogen bonds. The presented non-toxic nanodiamond treatment of flax can

be directly applied to make textiles more durable. It also shows great potential for improving flax as composite reinforcement. This needs to be verified in additional experiments.

Electronic supplementary material

The online version contains supplementary material.

Supporting Information This file contains extra figures and details about the calculation of the nanodiamond density and the DLVO model used.

Acknowledgments Carsten Hinzmann would like to thank Prof. Ignaas Verpoest for the useful discussion of this work at the ICCM23 in Belfast, United Kingdom. The authors are very grateful to the reviewers for their valuable feedback. This project was funded by Equinor through the Akademiaavtale program at the University of Bergen. Additional support was provided by the Faculty of Mathematics and Natural Science, University of Bergen.

Author contributions Carsten Hinzmann, Justas Zalieckas and Bodil Holst formulated the study concept and design. Material preparation, experiments, data collection, analysis and visualization were performed by Carsten Hinzmann. Modelling and calculation of the electrolytic force was performed by Drew F. Parsons. Modelling and calculation of the dispersion force was performed by Johannes Fiedler. The original draft of the manuscript was written by Carsten Hinzmann. Supervision, review & editing was performed by Justas Zalieckas and Bodil Holst. Project funding was acquired by Joachim Reuder, Justas Zalieckas and Bodil Holst. All authors commented on previous versions of the manuscript. All authors read and approved the final manuscript.

Funding Open access funding provided by University of Bergen (incl Haukeland University Hospital).

Data and code availability There is no extra data or code available.

Declarations

Conflict of interest On behalf of all authors, the corresponding author states that there is no conflict of interest.

Human and animal rights There are no experiments involving human tissue in this work.

References

Alongi J, Malucelli G (2013) Thermal stability, flame retardancy and abrasion resistance of cotton and cotton-linen blends treated by sol-gel silica coatings containing alumina micro- or nano-particles. Polym Degrad Stab 98(8):1428–1438. https://doi.org/10.1016/j.polymdegradstab.2013.05.002

Ansell MP, Mwaikambo LY (2009) 2 - The structure of cotton and other plant fibres. In: Eichhorn SJ, Hearle JWS, Jaffe M, Kikutani T (eds) Handbook of textile fibre structure, Woodhead publishing series in textiles, vol 2. Woodhead Publishing, Cambridge, pp 62–94. https://doi.org/10.1533/9781845697310.1.62

Arnault J, Girard H (2017) Hydrogenated nanodiamonds: synthesis and surface properties. Curr Opin Solid State Mater Sci 21(1):10–16. https://doi.org/10.1016/j.cossms.2016.06.007

Aslan M, Chinga-Carrasco G, Sørensen BF, Madsen B (2011) Strength variability of single flax fibres. J Mater Sci 46(19):6344–6354. https://doi.org/10.1007/s10853-011-5581-x

Baets J, Plastria D, Ivens J, Verpoest I (2014) Determination of the optimal flax fibre preparation for use in unidirectional flax-epoxy composites. J Reinf Plast Compos 33(5):493–502. https://doi.org/10.1177/0731684413518620

Baley C, Le Duigou A, Morvan C, Bourmaud A (2018) 8 - Tensile properties of flax fibers (2nd edn). The Textile Institute Book Series. In: Bunsell AR (ed) Handbook of properties of textile and technical fibres. Woodhead Publishing, Cambridge, pp 275–300. https://doi.org/10.1016/B978-0-08-101272-7.00008-0

Barella A (1950) Law of critical yarn diameter and twist influence on yarn characteristics. Text Res J 20(4):249–258. https://doi.org/10.1177/004051755002000405

Bergström L (1997) Hamaker constants of inorganic materials. Adv Colloid Interface Sci 70:125–169

Bismarck A, Aranberri-Askargorta I, Springer J, Lampke T, Wielage B, Stamboulis A, Shenderovich I, Limbach HH (2002) Surface characterization of flax, hemp and cellulose fibers; surface properties and the water uptake behavior. Polym Compos 23(5):872–894. https://doi.org/10.1002/pc.10485

Bos HL, Van Den Oever MJA, Peters OCJJ (2002) Tensile and compressive properties of flax fibres for natural fibre reinforced composites. J Mater Sci 37(8):1683–1692. https://doi.org/10.1023/A:1014925621252

Brodowsky HM, Hennig A (2021) Micromechanical tests on natural fibre composites with enzymatically enhanced

fibre-matrix adhesion. Mater Circ Econ 4(1):5. https://doi.org/10.1007/s42824-021-00040-4

Burger FA, Corkery RW, Buhmann SY, Fiedler J (2020) Comparison of theory and experiments on van der Waals forces in media-a survey. J Phys Chem C 124(44):24179–24186. https://doi.org/10.1021/acs.jpcc.0c06748

Carus M, Eder A, Dammer L, Korte H, Scholz L, Essel R, Breitmayer E, Barth M (2015) Wood-plastic composites (WPC) and natural fibre composites (NFC). Nova-Institute, Hürth

Charlet K, Eve S, Jernot JP, Gomina M, Breard J (2009) Tensile deformation of a flax fiber. Proc Eng 1(1):233–236. https://doi.org/10.1016/j.proeng.2009.06.055

Cicala G, Velardi L, Palazzo G, Valentini A, Perna G, Capozzi V (2017) Comparison between photoemitting and colloidal properties of nanodiamond particles. Colloids Surf A Physicochem Eng Aspects 532:493–500. https://doi.org/10.1016/j.colsurfa.2017.04.018

Cintrón MS, Johnson GP, French AD (2017) Quantum mechanics models of the methanol dimer: Oh-o hydrogen bonds of beta-d-glucose moieties from crystallographic data. Carbohydr Res 443–444:87–94. https://doi.org/10.1016/j.carres.2017.03.007

Derjaguin BV, Landau LD (1941) Theory of the stability of strongly charged lyophobic sols and of the adhesion of strongly charged particules in solution of electrolytes. Acta Physicochim URSS 14(6):633–662

Fiedler J, Thiyam P, Kurumbail A, Burger FA, Walter M, Persson C, Brevik I, Parsons DF, Boström M, Buhmann SY (2017) Effective polarizability models. J Phys Chem A 121(51):9742–9751. https://doi.org/10.1021/acs.jpca.7b10159

Fiedler J, Parsons DF, Burger FA, Thiyam P, Walter M, Brevik I, Persson C, Buhmann SY, Boström M (2019) Impact of effective polarisability models on the near-field interaction of dissolved greenhouse gases at ice and air interfaces. Phys Chem Chem Phys 21:21296–21304. https://doi.org/10.1039/C9CP03165K

Fiedler J, Berland K, Spallek F, Brevik I, Persson C, Buhmann SY, Boström M (2020a) Nontrivial retardation effects in dispersion forces: from anomalous distance dependence to novel traps. Phys Rev B 101:235424. https://doi.org/10.1103/PhysRevB.101.235424

Fiedler J, Boström M, Persson C, Brevik I, Corkery R, Buhmann SY, Parsons DF (2020b) Full-spectrum high-resolution modeling of the dielectric function of water. J Phys Chem B 124(15):3103–3113. https://doi.org/10.1021/acs.jpcb.0c00410

Fiedler J, Berland K, Borchert JW, Corkery RW, Eisfeld A, Gelbwaser-Klimovsky D, Greve MM, Holst B, Jacobs K, Krüger M, Parsons DF, Persson C, Presselt M, Reisinger T, Scheel S, Stienkemeier F, Tømterud M, Walter M, Weitz RT, Zalieckas J (2023) Perspectives on weak interactions in complex materials at different length scales. Phys Chem Chem Phys 25(4):2671–2705. https://doi.org/10.1039/D2CP03349F

Flatabø R, Coste A, Greve M (2017) A systematic investigation of the charging effect in scanning electron microscopy for metal nanostructures on insulating substrates. J Microsc 265(3):287–297. https://doi.org/10.1111/jmi.12497

Fukuzumi H, Tanaka R, Saito T, Isogai A (2014) Dispersion stability and aggregation behavior of tempo-oxidized cellulose nanofibrils in water as a function of salt addition. Cellulose 21:1553–1559. https://doi.org/10.1007/s10570-014-0180-z

Goutianos S, Peijs T (2003) The optimisation of flax fibre yarns for the development of high-performance natural fibre composites. Adv Compos Lett 12(6):096369350301200602. https://doi.org/10.1177/096369350301200602

Hartmann R, Kinnunen P, Illikainen M (2018) Cellulose-mineral interactions based on the dlvo theory and their correlation with flotability. Miner Eng 122:44–52. https://doi.org/10.1016/j.mineng.2018.03.023

Houshyar S, Nayak R, Padhye R, Shanks RA (2019) Fabrication and characterization of nanodiamond coated cotton fabric for improved functionality. Cellulose 26(9):5797–5806. https://doi.org/10.1007/s10570-019-02479-w

Hu L, Pasta M, La Mantia F, Cui L, Jeong S, Deshazer HD, Choi JW, Han SM, Cui Y (2010) Stretchable, porous, and conductive energy textiles. Nano Lett 10(2):708–714. https://doi.org/10.1021/nl903949m

Huda M, Drzal L, Ray D, Mohanty A, Mishra M (2008) 7 - Natural-fiber composites in the automotive sector. In: Pickering KL (ed) Properties and performance of natural-fibre composites, woodhead publishing series in composites science and engineering. Woodhead Publishing, Cambridge, pp 221–268. https://doi.org/10.1533/9781845694593.2.221

Hüster-Plogmann H, Schibler J, Jacomet S, Brombacher C, Gross-Klee E, Rast-Eicher A (1997) ökonomie und Ökologie neolithischer und bronzezeitlicher Ufersiedlungen am Zürichsee. Monographien der Kantonsarchäologie, Zürich

Joshi S, Drzal L, Mohanty A, Arora S (2004) Are natural fiber composites environmentally superior to glass fiber reinforced composites? Compos Part A Appl Sci Manuf 35(3):371–376. https://doi.org/10.1016/j.compositesa.2003.09.016

Karim N, Sarker F, Afroj S, Zhang M, Potluri P, Novoselov KS (2021) Sustainable and multifunctional composites of graphene-based natural jute fibers. Adv Sustain Syst 5(3):2000228. https://doi.org/10.1002/adsu.202000228

Khurshid MF, Hengstermann M, Hasan MMB, Abdkader A, Cherif C (2020) Recent developments in the processing of waste carbon fibre for thermoplastic composites—a review. J Compos Mater 54(14):1925–1944. https://doi.org/10.1177/0021998319886043

Kordkheili HY, Farsi M, Rezazadeh Z (2013) Physical, mechanical and morphological properties of polymer composites manufactured from carbon nanotubes and wood flour. Compos Part B Eng 44(1):750–755. https://doi.org/10.1016/j.compositesb.2012.04.023

Krüger A, Kataoka F, Ozawa M, Fujino T, Suzuki Y, Aleksenskii A, Vul' AY, Ōsawa E (2005) Unusually tight aggregation in detonation nanodiamond: identification and disintegration. Carbon 43(8):1722–1730. https://doi.org/10.1016/j.carbon.2005.02.020

Kumar S, Zindani D, Bhowmik S (2020) Investigation of mechanical and viscoelastic properties of flax- and ramie-reinforced green composites for orthopedic

implants. J Mater Eng Perform 29(5):3161–3171. https://doi.org/10.1007/s11665-020-04845-3
Leuzinger U, Rast-Eicher A (2011) Flax processing in the Neolithic and Bronze Age pile-dwelling settlements of eastern Switzerland. Veg Hist Archaeobot 20(6):535–542. https://doi.org/10.1007/s00334-011-0286-2
Li H, Tang R, Dai J, Wang Z, Meng S, Zhang X, Cheng F (2022) Recent Progress in Flax Fiber-Based Functional Composites. Adv Fiber Mater 4(2):171–184. https://doi.org/10.1007/s42765-021-00115-6
Li X, Tabil LG, Panigrahi S (2007) Chemical treatments of natural fiber for use in natural fiber-reinforced composites: A review. J Polym Environ 15(1):25–33. https://doi.org/10.1007/s10924-006-0042-3
Li Y, Chen C, Xu J, Zhang Z, Yuan B, Huang X (2015) Improved mechanical properties of carbon nanotubes-coated flax fiber reinforced composites. J Mater Sci 50(3):1117–1128. https://doi.org/10.1007/s10853-014-8668-3
Liang Y, Hilal N, Langston P, Starov V (2007) Interaction forces between colloidal particles in liquid: theory and experiment. Adv Colloid Interface Sci 134–135:151–166. https://doi.org/10.1016/j.cis.2007.04.003
Lu MM, Fuentes CA, Van Vuure AW (2022) Moisture sorption and swelling of flax fibre and flax fibre composites. Compos Part B Eng 231:109538. https://doi.org/10.1016/j.compositesb.2021.109538
Lukesova H, Holst B (2021) Is cross-section shape a distinct feature in plant fibre identification? Archaeometry 63(1):216–226. https://doi.org/10.1111/arcm.12604
da Luz FS, Garcia Filho FdC, del Río MTG, Nascimento LFC, Pinheiro WA, Monteiro SN (2020) Graphene-incorporated natural fiber polymer composites: a first overview. Polymers. https://doi.org/10.3390/polym12071601
Mandal S (2021) Nucleation of diamond films on heterogeneous substrates: a review. RSC Adv 11:10159–10182. https://doi.org/10.1039/D1RA00397F
Mccall RD, Kernaghan KJ, Sharma HSS (2001) Analysis of a crease-resisting finish on linen fabrics using Fourier transform infrared spectroscopy and visible and near-infrared spectroscopy. J Appl Polym Sci 82(8):1886–1896. https://doi.org/10.1002/app.2033
Mochalin VN, Shenderova O, Ho D, Gogotsi Y (2012) The properties and applications of nanodiamonds. Nat Nanotechnol 7(1):11–23. https://doi.org/10.1038/nnano.2011.209
Myllymäki V (2014) Monodispersed, highly zeta positive hydrogen terminated nanodiamond dispersion in water. https://www.carbodeon.com
Myllymäki V (2021) “hydrogen p and d” product - properties. https://www.carbodeon.com
Müssig J, Haag K (2015) 2 - the use of flax fibres as reinforcements in composites. In: Faruk O, Sain M (eds) Biofiber reinforcements in composite materials. Woodhead Publishing, Cambridge, pp 35–85. https://doi.org/10.1533/9781782421276.1.35
Naqvi S, Prabhakara HM, Bramer E, Dierkes W, Akkerman R, Brem G (2018) A critical review on recycling of end-of-life carbon fibre/glass fibre reinforced composites waste using pyrolysis towards a circular economy. Resour Conserv Recycl 136:118–129. https://doi.org/10.1016/j.resconrec.2018.04.013
Nishiyama Y (2018) Molecular interactions in nanocellulose assembly. Philos Trans R Soc A Math Phys Eng Sci 376(2112):20170047. https://doi.org/10.1098/rsta.2017.0047
Nurazzi NM, Asyraf MRM, Rayung M, Norrrahim MNF, Shazleen SS, Rani MSA, Shafi AR, Aisyah HA, Radzi MHM, Sabaruddin FA, Ilyas RA, Zainudin ES, Abdan K (2021) Thermogravimetric analysis properties of cellulosic natural fiber polymer composites: a review on influence of chemical treatments. Polymers. https://doi.org/10.3390/polym13162710
Peças P, Carvalho H, Salman H, Leite M (2018) Natural fibre composites and their applications: a review. J Compos Sci 2(4):2. https://doi.org/10.3390/jcs2040066
Pil L, Bensadoun F, Pariset J, Verpoest I (2016) Why are designers fascinated by flax and hemp fibre composites? Composites Part A: Applied Science and Manufacturing 83:193–205. https://doi.org/10.1016/j.compositesa.2015.11.004
Pusić T, Grancarić AM, Soljaçić I, Ribitsch V (1999) The effect of mercerisation on the electrokinetic potential of cotton. Color Technol 115(4):121–124. https://doi.org/10.1111/j.1478-4408.1999.tb00308.x
Rao Y, Farris RJ (2000) A modeling and experimental study of the influence of twist on the mechanical properties of high-performance fiber yarns. J Appl Polym Sci 77(9):1938–1949. https://doi.org/10.1002/1097-4628(20000829)77:9<1938::AID-APP9>3.0.CO;2-D
Rukuiziene Z, Kumpikaite E (2013) Investigation of initial warp tension and weave influence on warp yarn diameter projections. Fibres Text East Eur Nr 5(101):43–48
Sarker F, Karim N, Afroj S, Koncherry V, Novoselov KS, Potluri P (2018) High-performance graphene-based natural fiber composites. ACS Appl Mater Interfaces 10(40):34502–34512. https://doi.org/10.1021/acsami.8b13018.
Sarker F, Potluri P, Afroj S, Koncherry V, Novoselov KS, Karim N (2019) Ultrahigh performance of nanoengineered graphene-based natural jute fiber composites. ACS Appl Mater Interfaces 11(23):21166–21176. https://doi.org/10.1021/acsami.9b04696
Scheel S, Buhmann SY (2008) Macroscopic quantum electrodynamics—concepts and applications. ACTA Phys Slovaca 58(5):675–809. https://doi.org/10.2478/v10155-010-0092-x
Schmidlin L, Pichot V, Comet M, Josset S, Rabu P, Spitzer D (2012) Identification, quantification and modification of detonation nanodiamond functional groups. Diamond Relat Mater 22:113–117. https://doi.org/10.1016/j.diamond.2011.12.009
Shah DU, Schubel PJ, Licence P, Clifford MJ (2012) Hydroxyethylcellulose surface treatment of natural fibres: the new ‘twist’ in yarn preparation and optimization for composites applicability. J Mater Sci 47(6):2700–2711. https://doi.org/10.1007/s10853-011-6096-1
Shah DU, Schubel PJ, Clifford MJ (2013) Modelling the effect of yarn twist on the tensile strength of unidirectional plant fibre yarn composites. J Compos Mater 47(4):425–436. https://doi.org/10.1177/0021998312440737

Shen X, Jia J, Chen C, Li Y, Kim JK (2014) Enhancement of mechanical properties of natural fiber composites via carbon nanotube addition. J Mater Sci 49(8):3225–3233. https://doi.org/10.1007/s10853-014-8027-4

Siffert B, Metzger JM (1991) Study of the interaction of titanium dioxide with cellulose fibers in an aqueous medium. Colloids Surf 53:79–99. https://doi.org/10.1016/0166-6622(91)80037-O

Stamboulis A, Baillie C, Peijs T (2001) Effects of environmental conditions on mechanical and physical properties of flax fibers. Compos Part A Appl Sci Manuf 32(8):1105–1115. https://doi.org/10.1016/S1359-835X(01)00032-X

Stehlik S, Glatzel T, Pichot V, Pawlak R, Meyer E, Spitzer D, Rezek B (2016) Water interaction with hydrogenated and oxidized detonation nanodiamonds—microscopic and spectroscopic analyses. Diamond Relat Mater 63:97–102. https://doi.org/10.1016/j.diamond.2015.08.016

Surina R, Andrassy M (2013) Effect of preswelling and ultrasound treatment on the properties of flax fibers cross-linked with polycarboxylic acids. Text Res J 83(1):66–75. https://doi.org/10.1177/0040517512452928

Sychev DY, Zhukov AN, Golikova EV, Sukhodolov NG (2017) The effect of simple electrolytes on coagulation of hydrosols of monodisperse negatively charged detonation nanodiamond. Colloid J 79:822–828. https://doi.org/10.1134/S1061933X17060163

Thiyam P, Persson C, Parsons D, Huang D, Buhmann S, Boström M (2015) Trends of co2 adsorption on cellulose due to van der Waals forces. Colloids Surf A Physicochem Eng Aspects 470:316–321. https://doi.org/10.1016/j.colsurfa.2014.12.044

Tzounis L, Debnath S, Rooj S, Fischer D, Mäder E, Das A, Stamm M, Heinrich G (2014) High performance natural rubber composites with a hierarchical reinforcement structure of carbon nanotube modified natural fibers. Mater Design 58:1–11. https://doi.org/10.1016/j.matdes.2014.01.071

Van Langenhove L (1997) Simulating the mechanical properties of a yarn based on the properties and arrangement of its fibers part II: results of simulations. Text Res J 67(5):342–347. https://doi.org/10.1177/004051759706700506

Van de Velde K, Baetens E (2001) Thermal and mechanical properties of flax fibres as potential composite reinforcement. Macromol Mater Eng 286(6):342–349. https://doi.org/10.1002/1439-2054(20010601)286:6<342::AID-MAME342>3.0.CO;2-P

Vervald AM, Laptinskiy KA, Burikov SA, Laptinskaya TV, Shenderova OA, Vlasov II, Dolenko TA (2019) Nanodiamonds and surfactants in water: hydrophilic and hydrophobic interactions. J Colloid Interface Sci 547:206–216. https://doi.org/10.1016/j.jcis.2019.03.102

Verwey EJW, Overbeek JTG (1948) Theory of the stability of lyophobic colloids. Elsevier, Amsterdam

Vul AY, Dideikin AT, Aleksenskii AE, Baidakova MV (2014) Detonation nanodiamonds: synthesis, properties and applications. In: Nanodiamond, Royal Society of Chemistry Cambridge, UK, chap 2.2, pp 33–35. https://doi.org/10.1039/9781849737616-00027

Van de Weyenberg I, Chi Truong T, Vangrimde B, Verpoest I (2006) Improving the properties of UD flax fibre reinforced composites by applying an alkaline fibre treatment. Compos Part A Appl Sci Manuf 37(9):1368–1376. https://doi.org/10.1016/j.compositesa.2005.08.016

Williams OA, Douhéret O, Daenen M, Haenen K, Ōsawa E, Takahashi M (2007) Enhanced diamond nucleation on monodispersed nanocrystalline diamond. Chem Phys Lett 445(4):255–258. https://doi.org/10.1016/j.cplett.2007.07.091

Williams OA, Hees J, Dieker C, Jäger W, Kirste L, Nebel CE (2010) Size-dependent reactivity of diamond nanoparticles. ACS Nano 4(8):4824–4830. https://doi.org/10.1021/nn100748k

Wohlert M, Benselfelt T, Wågberg L, Furó I, Berglund LA, Wohlert J (2022) Cellulose and the role of hydrogen bonds: not in charge of everything. Cellulose 29(1):1–23. https://doi.org/10.1007/s10570-021-04325-4

Wu Y, Xia C, Cai L, Garcia AC, Shi SQ (2018) Development of natural fiber-reinforced composite with comparable mechanical properties and reduced energy consumption and environmental impacts for replacing automotive glass-fiber sheet molding compound. J Clean Prod 184:92–100. https://doi.org/10.1016/j.jclepro.2018.02.257

Yoshikawa T, Zuerbig V, Gao F, Hoffmann R, Nebel CE, Ambacher O, Lebedev V (2015) Appropriate salt concentration of nanodiamond colloids for electrostatic self-assembly seeding of monosized individual diamond nanoparticles on silicon dioxide surfaces. Langmuir 31(19):5319–5325. https://doi.org/10.1021/acs.langmuir.5b01060

Zhang C, Keten S, Derome D, Carmeliet J (2021) Hydrogen bonds dominated frictional stick-slip of cellulose nanocrystals. Carbohydr Polym 258:117682. https://doi.org/10.1016/j.carbpol.2021.117682